Nuclear Instruments and Methods in Physics Research B 498 (2021) 34–38

Contents lists available at ScienceDirect

Nuclear Inst. and Methods in Physics Research, B

journal homepage: www.elsevier.com/locate/nimb

The comparison of bulk and in-situ irradiation damage on cubic-Lu_2TiO_5 and orthorhombic-La_2TiO_5

Huanhuan He [a], Qiurong Xie [a], Zhiwei Lin [a], Shengming Jiang [a], Xiaotian Hu [a], Ming Tang [b,c,*], Jian Zhang [a,*]

[a] College of Energy, Xiamen University, Xiamen, Fujian 361005, China
[b] Department of Materials Science and Engineering, Clemson University, Clemson, SC 29631, USA
[c] Center for Nuclear Environmental Engineering Sciences and Radioactive Waste Management (NEESRWM), Clemson University, Clemson, SC, USA

ARTICLE INFO

Keywords:
In-situ ion irradiation
Ex-situ ion irradiation
Amorphization

ABSTRACT

Polycrystalline cubic-Lu_2TiO_5 and orthorhombic-La_2TiO_5 compounds were prepared by traditional ceramic processing. In-situ and ex-situ ion beam irradiations were performed on these samples at room temperature. Bulk samples were irradiated with 800 keV Kr^{2+} ions and characterised ex-situ, whilst powder samples were in-situ irradiated with 1 MeV Kr^{2+} ions. For Lu_2TiO_5, a completely amorphization was observed at the fluences of 2 $\times$ 10^{14} ions/cm^2 (~0.37 dpa) in the bulk sample and 5 $\times$ 10^{14} ions/cm^2 (~0.99 dpa) in the TEM sample. For La_2TiO_5, complete amorphization was observed at the fluences of 5 $\times$ 10^{13} ions/cm^2 (~0.08 dpa) in the bulk sample and 1.25 $\times$ 10^{14} ions/cm^2 (~0.21 dpa) in the TEM sample. It seems that a higher irradiation fluence to amorphization was needed for in-situ TEM samples than that for bulk samples.

1. Introduction

Polycrystalline pyrochlore Ln_2O_3-TiO_2 is considered as one of the potential nuclear waste immobilization matrices due to its good chemical stability and low leaching rate [1,2]. Radiation damage studies on this phase has also attracted wide attention [3–5]. Ion beam irradiation is used to simulate the alpha decay radiation damage of the nuclear waste immobilization matrix [6]. According to previous research results, Ln_2O_3-TiO_2 doped with different ionic radii of Ln possess three different crystal structures (cubic, hexagonal and orthorhombic crystal system) [7]. Previous studies have revealed the crystalline-to-amorphizaton transformation on Ln_2O_3-TiO_2 by in-situ ion irradiation [8–12]. The critical temperature (Tc) for maintaining crystallinity of Ln_2O_3-TiO_2 doped with different lanthanide was studied using in-situ TEM observation [9]. Currently, Most of ion irradiation studies of the Ln_2O_3-TiO_2 samples have used the TEM coupled with in-situ ion-irradiation approach. There are few reports on the differences of ex-situ and in-situ irradiation approaches in the Ln_2O_3-TiO_2 samples. In addiation, the radiation behaviours of ion irradiated bulk and thin-foil tungsten have been studied [13], where a much higher dislocation loops are formed in TEM samples versus bulk samples. Meanwhile, in the ultra high purity Fe samples, the number density of defects in TEM also is higher than in the bulk specimens [14,15]. The purpose of this study is to compare the thin-foil TEM samples (in-situ irradiation) and the bulk samples (ex-situ irradiation) under ion irradiation for Lu_2TiO_5 and La_2TiO_5 samples. Our experimental results can verify the universality of the differences at the cubic-Lu_2TiO_5 and the orthorhombic-La_2TiO_5 samples which possess similar chemical stoichiometry but different crystal structures. This study also provides a possible method and explanation to better compare and understand the irradiation results of the Ln_2O_3-TiO_2 compounds from the different research groups by using in-situ TEM and ex-situ bulk irradiation, repectively.

2. Material and methods

Polycrystalline pyrochlore cubic-Lu_2TiO_5 and orthorhombic-La_2TiO_5 samples were prepared by traditional standard solid sintering. The Lu_2O_3, La_2O_3 (99.99% purity, HWRK CHEM, China) and TiO_2 (99.99% purity, HWRK CHEM, China) powders were first heated at 1273 K for 10 h to remove moisture and other volatile impurities. The above powders were weighed based on the 1: 1 mol ratio, ball-milled for 4 h, and cold pressed into pellets. Then these pellets were sintered at 1473 K in air for 24 h. To obtain a better homogeneity and compactness, the samples were reground, cold pressed, and sintered once again at 1673 K for 48 h.

* Corresponding authors at: Department of Materials Science and Engineering, Clemson University, Clemson, SC 29631, USA (M. Tang).
E-mail addresses: mingt@clemson.edu (M. Tang), zhangjian@xmu.edu.cn (J. Zhang).

https://doi.org/10.1016/j.nimb.2021.04.017
Received 12 January 2021; Received in revised form 5 April 2021; Accepted 21 April 2021
Available online 4 May 2021

The measured densities of the final Lu_2TiO_5 and La_2TiO_5 are 7.48 and 5.16 g/cm^3, corresponding to 95.3% and 94.2% of the theoretical densities, respectively. The samples were cut into 1 mm thick pellet which are polished to 1 μm finish for the bulk ex-situ ion irradiation experiment. The ~1 mm thick bulk samples were irradiated with 800 keV Kr^{2+} ions at room temperature using the NEC-400 kV ion implanter in Xiamen University. The irradiation fluences range from 5×10^{12} to 2×10^{14} ions/cm^2. The 800 keV Kr^{2+} ions irradiation flux, with the raster beam of half width ~1 cm, was kept lower to ~8×10^{11} Kr^{2+} /cm^2/s $8 \times 10^{11}$$Kr^{2+}$/cm^{2}to minimise the beam heating effects. The ion irradiated bulk samples were characterized by grazing incidence X-ray diffraction (GIXRD) (Rigaku Ultima IV Advanced X-ray diffractometer). The diffractometer was operated in a θ-2θ geometry with the 2θ range of 10-70° and a step size of 0.02°with Cu Kα ($\lambda = 0.15406$ nm) radiation. The incident angle of X-rays was fixed at 0.5°, where the penetration depth of the X-ray was below 100 nm, so the X-ray diffraction data was obtained from the irradiation damage layer.

In-situ TEM irradiation was performed using the intermediate voltage electron microscope (IVEM)-Tandem facility at Argonne National Laboratory with 1 MeV Kr^{2+} beam at room temperature. TEM specimens were irradiated at 30°normal angle off the electron beam direction. The ion flux was kept at constant (~6.25×10^{11} ions/ cm^2/s) to minimize the heating effect. The bulk samples were milled to power, then dispensed in the carbon-coated Cu TEM grids to get the powder TEM specimens. During the ion irradiation, the TEM electron beam valve was closed to avoid additional damage from the electron beam and the electron heating effects. The selected area electron diffraction (SAED) with an probing area ~ 100 nm was used to monitor the structure change with the irradiation dose increasing.

Meanwhile, the 800 keV and 1 MeV Kr^{2+} ions ranges and damage depth profile in the samples are evaluated by using the stopping range of ions in matter (SRIM) code with simple Kinchin-Pease model (arbitrarily assumed the threshold displacement energies of all elements are 40 eV). The examined depth of GIXRD is similar to the thickness of SAED (~100 nm). While, the SRIM simulation shows that the displacement damage peaks are at ~200 nm for both samples (Table 1).

3. Results

Fig. 1 shows the GIXRD patterns of pristine Lu_2TiO_5 and Lu_2TiO_5 irradiated with 800 keV Kr^{2+} at the fluences ranging from 5×10^{12} to 2×10^{14} ions/cm^2 at room temperature. The primary $(111)_c$ reflection of the cubic structure is shifted towards lower 2θ angle at a fluence of 5×10^{12} ions/cm^2, which indicates lattice swelling during the irradiations. With increasing irradiation fluence, the crystal reflections intensity decrease obviously and an amorphization diffraction shows up around the $(111)_c$ and $(200)_c$ reflection. The GIXRD results reveal that a crystalline to amorphization phase transformation is initiated at the irradiation fluence of 2×10^{13} ions/cm^2 and is fully amorphous at the fluence of 2×10^{14} ions/cm^2. No intermediate phase is observed during irradiation.

The in-situ SAED patterns of Lu_2TiO_5 irradiated at different fluences

Table 1
SRIM simulation results for 800 keV Kr^{2+} ions irradiation on bulk samples and 1 MeV Kr^{2+} ions irradiation on in-situ samples to a fluence of 1.0×10^{14} ions/cm^2.

Sample	Lu_2TiO_5		La_2TiO_5	
	Bulk sample	In-situ sample	Bulk sample	In-situ sample
Ion range (nm)	670	730	740	890
Damage peak depth (nm)	150	170	200	190
Peak damage (dpa)	0.19	0.21	0.18	0.19
Surface (~100 nm) damage (dpa)	0.18	0.19	0.15	0.17
Ion concentration (ppm)	49.76	40.86	54.52	45.95

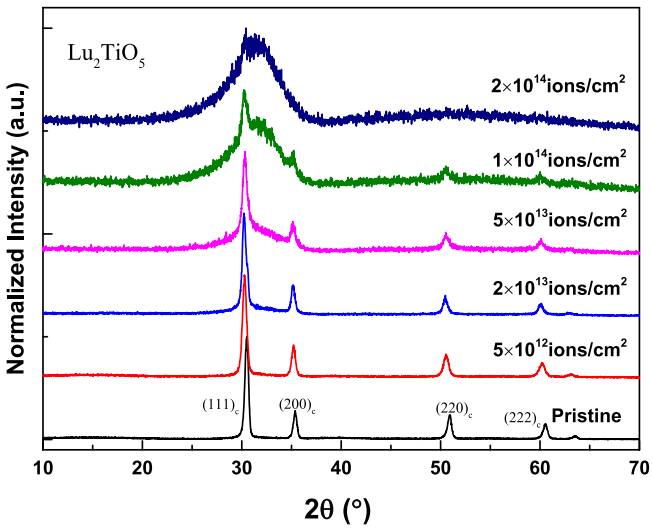

Fig. 1. The GIXRD patters of pristine Lu_2TiO_5 and Lu_2TiO_5 irradiated with 800 keV Kr^{2+} from 5×10^{12} to 2×10^{14} ions/cm^2.

are shown in Fig. 2. Based on the diffraction patterns, the sample starts with cubic structure through the electron beam along the [011] direction, shown in Fig. 2(a), (b). As the radiation fluence is increasing, the diffraction patterns show the appearance of an amorphous halo accompanied by clearly visible diffraction spots in Fig. 2(c), (d), which reveals the co-existence of the crytalline and amorphous phases during the irradiation. Further ion irradiation cause the crystalline spots to completely disappear with only the amorphous halo remaining in Fig. 2 (e), which suggest full amorphization at 5.0×10^{14} ions/cm^2. The diffuse ring runs through the diffraction spots of (200) and (1–11) corresponding to the result of GIXRD where an amorphous diffraction halo appears at the characteristic peaks of $(111)_c$ and $(200)_c$. Experimental results reveal that, higher radiation dose is needed to achieve fully amorphization in the in-situ irradiated sample when compared to the ex-situ sample.

GIXRD pattern in Fig. 3 shows that the pristine La_2TiO_5 sample possesses an orthorhombic phase. X-ray diffraction data of the irradiated samples shows a tendency to amorphization with the increase of fluence. When the fluences increase to 2×10^{13} ions/cm^2, except the characteristic peaks of $(210)_o$ and $(203)_o$, other diffraction peaks disappear, so we understand it is close to fully amorphous. As the fluence is increased to 5×10^{13} ions/cm^2, all characteristic peaks disappear, only leaving a diffraction halo around $2\theta = 30°$, which indicates complete amorphization. Based on the GIXRD observations of both La_2TiO_5 and Lu_2TiO_5, the latter exhibits greater resistance to amorphization.

An in-situ irradiation-induced amorphization process is also observed in La_2TiO_5 sample in Fig. 4. The pristine SAED pattern is indexed as the orthorhombic system with the electron beam along the [27–3] direction. The diffraction pattern at the fluence of 2.5×10^{13} ions/cm^2 shows almost no changes, while an amorphous ring appears at the fluence of 5×10^{13} ions/cm^2, as shown in Fig. 4(b), (c). As the radiation fluence increases, the amorphous ring becomes brighter and the diffraction maxima are dimmer, which suggests that the fraction of amorphous phase increases. When the irradiation fluence reaches 1.25×10^{14} ions/cm^2 in Fig. 4(e), the diffraction spots almost completely disappear, indicating that the sample is close to fully amorphous. Also, the diffuse ring run through the diffraction spots of (302). Compared with the corresponding ex-situ GIXRD results, the in-situ irradiated La_2TiO_5 is fully amorphized at a higher radiation fluence, which is consistent with the observation on Lu_2TiO_5.

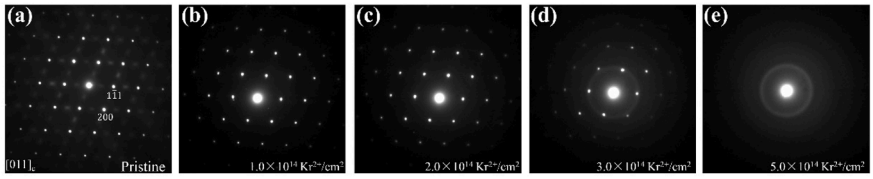

Fig. 2. Sequences of SAED patterns of pristine Lu_2TiO_5 and Lu_2TiO_5 at increasing ion fluences irradiated at room temperature along [011] direction.

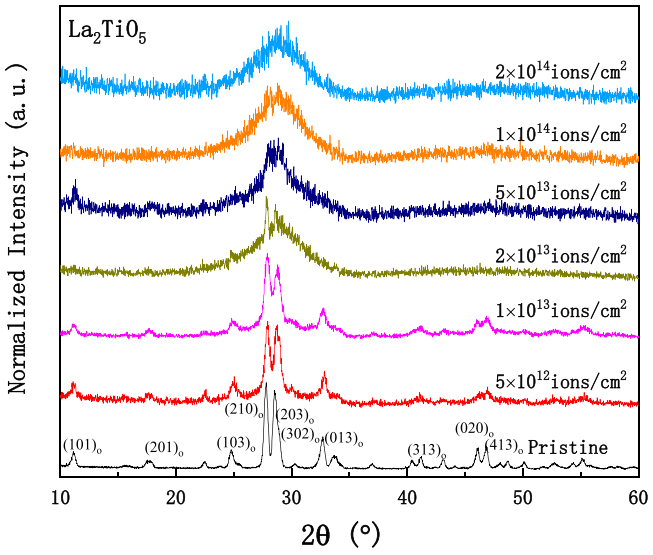

Fig. 3. The GIXRD patters of pristine La_2TiO_5 and La_2TiO_5 irradiated with 800 keV Kr^{2+} from 5×10^{12} to 2×10^{14} ions/cm^2.

4. Discussion

The experimental results show that full amorphization occurs at a higher fluence for ion-irradiated Lu_2TiO_5 and La_2TiO_5 samples under in-situ Kr irradiation when compared with ex-situ irradiation. In order to understand the dose difference, the amorphous fractions in different samples are plotted and fitted with fluences (Fig. 5). The amorphous fractions are fitted based on the classical relation further extended by Gibbons [16]:

$$f_a = 1 - \sum_{n=0}^{m-1} \frac{(V \cdot D)^n}{n!} e^{-V \cdot D} \quad (1)$$

where f_a is the amorphous fraction, V is the average survived damage area per ion after the defects moved and annihilated, D is the dose (ions per unit volume). The formula suggests that the overlap of collision cascades lead to irradiation induced amorphization. The value of m is the overlapping number of collision cascades required to create an amorphous volume, which relates to the survived defects density and the free energy discrepency between crystalline and amorphous structure. If $m = 1$, the formula becomes $f_a = 1 - e^{-V \cdot D}$, indicating a direct amorphous process which occurs at a single cascade. The amorphization process will be determined by the V and m together.

Fig. 5 shows that the slopes of amorphous fraction as a function of fluences for ex-situ and in-situ irradiated samples are very different. The in-situ amorphous fractions are calculated from SAED images. EDP2XRD code is used to convert electron diffraction rings pattrerns into X-ray diffraction patterns [17]. After removing the background, the different intensities of the amorphous ring and diffraction spots are measured and then normalized to the intensity of fully amorphous ring [18]. Attention has been paid so that the SAED images of each sample are obtained from the same position and the same orientation for each grain.

As shown in Fig. 5(a), the amorphous fractions of the bulk Lu_2TiO_5 samples increase rapidly at the beginning of irradiation (low dose) and progress to complete amorphization. The fitting constants are calculated as $m = 2$ and $V = 3.42$ (see Table 2), which means two cascading

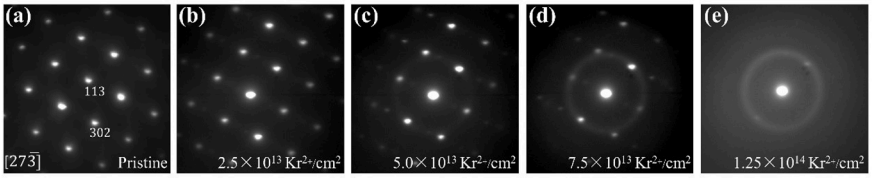

Fig. 4. Sequences of SAED patterns of pristine La_2TiO_5 and La_2TiO_5 at increasing ion fluences irradiated at room temperature along [27–3] direction.

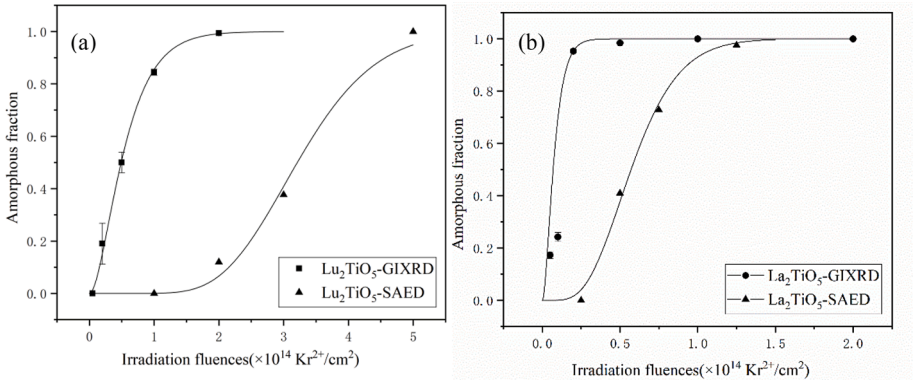

Fig. 5. The fitting curve of amorphous ratio with increasing irradiation influence in different samples (a) Lu_2TiO_5 and (b) La_2TiO_5.

collisions were needed to create an amorphous zone. The amorphization process is close to a direct impact process. By contrast, the in-situ Lu_2TiO_5 samples have a slowly increasing amorphous fraction in the early stage of irradiation, then increase rapidly, and finally tend to complete amorphization, corresponding to m = 12 and V = 3.63. It implies that 12 times cascading collisions overlap are required to create an amorphous zone, which suggests a process of defects accumulation [19]. With similar "V" values, the "m" value of the bulk Lu_2TiO_5 is much smaller than that of the in-situ samples, indicating that the concentration of defects retained in bulk Lu_2TiO_5 sample is higher and easier to become amorphous, which is in consistent with the results shown in Fig. 1 and Fig. 2.

In Fig. 5(b), the fitting constants are calculated as m = 7 and V = 61.27 in bulk La_2TiO_5 samples, while m = 5 and V = 9.93 in in-situ La_2TiO_5 samples (see Table 2). Here, the value of "m" is similar, and the difference can be regarded as a statistical discrepancy of data. With similar "m" values, the "V" value of the bulk La_2TiO_5 samples is much larger than that of the in-situ samples, indicating that the defect mobility of the bulk sample is smaller and the defect annihilates less, which leads to a faster amorphous process in bulk La_2TiO_5 sample.

Compared with the ex-situ bulk samples, the in-situ thin TEM foils are more resistant to amorphization in both two samples. This may be that a higher ratio of free surface to volume and a larger specific surface area in in-situ irradiation samples, surfaces can act as effective sinks for point defects of interstitials and vacancies and small mobile defect clusters, and thus significantly change defect diffusion kinetics and distribution profiles [20]. At the in-situ irradiation, more defects annihilate near the surfaces, and the survived defects is not enough to make the in-situ samples amorphous at the low irradation fluence in the surface domain. So, the in-situ samples have a slowly increasing amorphous fraction in the early stage of irradiation. In addition, the similar slow increasing curve of the amorphous versus irradiation fluences is reported for He irradation in the silicon via SAED [18]. Meanwhile, an obvious lower amorphous fraction is observed for Xe irradiation in the silicon at lower irradiation fluence via SAED [18]. It proves that the amorphous curve of the in-situ samples is affected by the surface effects.

In conclusion, the damage process to the sample in the in-situ irradiation experiment is quite different from that in the ex-situ irradiation experiment. The bulk sample of the ex-situ experiments may retain a larger concentration of defects at the same fluences compared the in-situ samples. In the in-situ condition, these defects may escape to the greater free surface available and disappear, so that the in-situ samples retains fewer defects at the same fluences as compared with bulk irradiated samples.

If we compare these two materials La_2TiO_5 and Lu_2TiO_5, the "V" value of the La_2TiO_5 samples is generally larger, indicating that the defect diffusion in the La_2TiO_5 sample is slower, so it is more susceptible to becoming amorphous. At the same irradiation conditions, the fluences required to reach complete amorphization for La_2TiO_5 is much less than that for Lu_2TiO_5. Because the element La possesses a larger ionic radius than Lu element, La_2TiO_5 and Lu_2TiO_5 crystallize in orthorhombic (Pnam) and cubic structures (Fd3m), respectively [21]. Previous studies reported that different Ln ionic radii affect the crystal structure formation of $Ln_2Ti_2O_7$ and Ln_2TiO_5 [9,10]. Our results indicate that as the Ln ionic radii decreases, the radiation resistance gradually increases, which may be due to a higher anti-site formation energy of larger Ln radius in the ion irradiation process [22]. For La_2TiO_5, the ion-irradiation results show a behaviour of direct amorphization due to the large difference of La and Ti ions in atomic radius and the high formation energy of anti-site defects. For Lu_2TiO_5, Lu and Ti ionic radii are the closest among Ln elements, so lower anti-site defects formation energy induced higher radiation tolerance to amorphization.

5. Conclusion

In summary, ex-situ 800 keV Kr^{2+} and in-situ 1 MeV Kr^{2+} ion irradiation damage experiments were conducted at room temperature on cubic Lu_2TiO_5 and orthorhombic La_2TiO_5. Both the ex-situ and in-situ irradiated Lu_2TiO_5 samples undergo a gradually increasing amorphous fraction with fluence and eventually complete amorphization with increasing fluences. Similar radiation-induced microstructural evolution is obtained in La_2TiO_5 samples. At the same time, the samples under the in-situ irradiation are more resistant to amorphization than the bulk samples under ex-situ irradiation. Our experimental results reveal different amorphization mechanisms in ex-situ and in-situ experiments. The direct impact model could be used to explain amorphization process in ex-situ irradiated samples, while a defects accumulation model is more suitable for in-situ irradiated samples. The samples of Lu_2TiO_5 show greater resistance to amorphiztion when compared with La_2TiO_5 due to the lower anti-site defects formation energy.

Table 2
Fitting parameters for different samples at different irradiation conditions.

Sample	Lu_2TiO_5		La_2TiO_5	
	Bulk sample	In-situ sample	Bulk sample	In-situ sample
Fitting value of "m"	2	12	7	5
Fitting value of "V"	3.42	3.63	61.27	9.93
R-squared	0.999008	0.994417	0.985881	0.997979

CRediT authorship contribution statement

Huanhuan He: Writing - original draft, Formal analysis, Software, Methodology. **Qiurong Xie:** Investigation. **Zhiwei Lin:** Writing - review & editing. **Shengming Jiang:** Writing - review & editing. **Xiaotian Hu:** Writing - review & editing. **Ming Tang:** Writing - review & editing, Resources, Supervision. **Jian Zhang:** Funding acquisition, Project administration, Supervision, Conceptualization.

Declaration of competing interest

The authors declare that they have no known competing financial interests or personal relationships that could have appeared to influence the work reported in this paper.

Acknowledgements

The authors are grateful for the financial support from the National Natural Science Foundation of China (Grant No.12075200), and partial support from the Joint Funds of the Natural Science Foundation of China (Grant No. U1967206) and Educational Research Projects of Fujian, China (Grant No. KL41830).

MT would like to thank the U.S. Department of Energy, Office of Nuclear Energy for long time support under Fuel Cycle Technology Program, Materials Recovery and Waste Form Campaign.

MT also accknowledge the partly funded professorship by the U.S. Nuclear Regulatory Commission.

The electron microscopy with in situ ion irradiation was accomplished at Argonne National Laboratory at the IVEM-Tandem Facility, a Nuclear Science User Facility funded by the U.S. Department of Energy, Office of Nuclear Energy, operated under Contract no.D E-AC02–06CH11357 by UChicago Argonne, LLC.

References

[1] H.F. Xu, Y.F. Wang, P.H. Zhao, W.L. Bourcier, R. Van Konynenburg, H.F. Shaw, Environ. Sci. Technol. 38 (2004) 1480–1486.
[2] S.V. Yudintsev, S.V. Tomilin, T.S. Livshits, A.A. Lizin, I.A. Goryatchev, Dokl. Earth Sci. 469 (2016) 732–736.
[3] Q.-R. Xie, J. Zhang, D.-M. Yin, Q.-X. Guo, N. Li, Chin. Phys. B 24 (2015).

[4] Q.R. Xie, J. Zhang, X.N. Dong, Q.X. Guo, N. Li, J. Solid State Chem. 231 (2015) 159–162.
[5] J. Zhang, Q.R. Xie, X.N. Dong, X.L. Jiao, N. Li, Nucl. Instrum. Methods Phys. Res. B 441 (2019) 88–92.
[6] X.Y. Shu, L. Fan, Y. Xie, W.D. Zhu, S.Q. Pan, Y. Ding, F.T. Chi, Y.L. Wu, X.R. Lu, J. Eur. Ceram. Soc. 37 (2017) 779–785.
[7] Y.F. Shepelev, M.A. Petrova, Inorg. Mater. 44 (2008) 1354–1361.
[8] K.R. Whittle, G.R. Lumpkin, M.G. Blackford, R.D. Aughterson, K.L. Smith, N. J. Zaluzec, J. Solid State Chem. 183 (2010) 2416–2420.
[9] R.D. Aughterson, G.R. Lumpkin, M. Ionescu, M.d.l. Reyes, B. Gault, K.R. Whittle, K. L. Smith, J.M. Cairney, J. Nucl. Mater., 467, Part 2 (2015) 683-691.
[10] J. Zhang, F. Zhang, M. Lang, F. Lu, J. Lian, R.C. Ewing, Acta Mater. 61 (2013) 4191–4199.
[11] R.D. Aughterson, G.R. Lumpkin, K.L. Smith, Z.M. Zhang, N. Sharma, J.M. Cairney, Ceram. Int. 44 (2018) 511–519.
[12] X. Liu, D.Y. Yang, C.G. Liu, H. Liu, S.Y. Ji, P.C. Mu, Y.Y. Wu, Y.H. Li, Comput. Mater. Sci. 139 (2017) 295–300.
[13] R.-Y. Zheng, W.-Z. Han, Acta Mater. 186 (2020) 162–171.
[14] A. Prokhodtseva, B. Décamps, R. Schäublin, J. Nucl. Mater. 442 (2013) S786–S789.
[15] K. Xu, M.H. Weber, Y. Cao, W. Jiang, D.J. Edwards, B.R. Johnson, J.S. McCloy, J. Nucl. Mater. 526 (2019), 151774.
[16] J.F. Gibbons, Microelectron Reliab 12 (1973) 216.
[17] H. Liu, M. Foley, Q. Lin, J. Liu, J. Appl. Crystallogr. 49 (2016) 636–641.
[18] P.D. Edmondson, K.J. Abrams, J.A. Hinks, G. Greaves, C.J. Pawley, I. Hanif, S. E. Donnelly, Scripta Mater. 113 (2016) 190–193.
[19] W.J. Weber, Nucl. Instrum. Methods Phys. Res. B 166–167 (2000) 98–106.
[20] M.M. Li, M.A. Kirk, P.M. Baldo, D.H. Xu, B.D. Wirth, Philos. Mag. 92 (2012) 2048–2078.
[21] F.X. Zhang, J.W. Wang, M. Lang, J.M. Zhang, R.C. Ewing, J. Solid State Chem. 183 (2010) 2636–2643.
[22] K.E. Sickafus, L. Minervini, R.W. Grimes, J.A. Valdez, M. Ishimaru, F. Li, K. J. McClellan, T. Hartmann, Science 289 (2000) 748–751.